Numerical tools for the mesoscale modeling of thermostructural woven composites

C. Fagiano, Emmanuel Baranger, P. Ladeveze, Martin Genet

Numerical tools for the mesoscale modeling of thermostructural woven composites.

C. Fagiano[1*], E. Baranger[1], P. Ladevèze[1,2], M. Genet[3]

[1]*LMT-Cachan, ENS-Cachan /CNRS/UPMC/PRES UniverSud Paris, 61 avenue du Président Wilson, 94235 Cachan Cedex, France*
[2]*EADS Foundation Chair ''Advanced Computational Structural Mechanics'', France*
[3]*Lawrence Berkeley National Laboratory, One Cyclotron Road, Berkeley, CA-94720, USA*
**fagiano@lmt.ens-cachan.fr*

Keywords: Thermostructural woven composites, mesoscale modeling, damage mechanics.

Abstract

Thermostructural woven composite materials are receiving particular attention in a wide range of specialized aeronautical applications. Reliable numerical prediction tools based on both geometrical and mechanical modeling are required to quantitatively characterize the role of the microstructure and damage mechanisms at the mesoscale. In this paper, a finite element strategy is proposed illustrating a generic two-dimensional repeating unit cell of a SiC/SiC plain weave composite with chemical vapor infiltrated matrix. Tows damage mechanisms are introduced through a nonlinear model based on damage mechanics as well as homogenization of a micromechanical model on the fiber scale. Particular attention is paid to the generation of accurate hexahedral meshes, compatible at the tow-tow and tow-matrix interfaces. The mesh quality is verified using an error estimator variable based on the strain energy density. Intra-yarn damage prediction obtained using tetrahedral and hexahedral elements is tested and compared considering the representative unit cell subjected to tensile loading.

1 Introduction

Composite materials manufactured using textile architectures are receiving a growing interest in the field of advanced structural applications [1]. One of the reasons is related to the fact that the microstructure of fiber preforms can be tailored to satisfy the specific needs for mechanical performance. The advantages include also the ease of handling for automation, the ability to conform complex shapes, thicker fiber forms, and virtual elimination of interlaminar surfaces through the fully integrated fiber arrangement making them less sensible to delamination effects. However, their mechanical in-plane properties, stiffness as well as strength, are lower than those of UD-composites. The reason for this drawback is the generally higher fiber undulation, which is due to the textile fiber architecture and to the fabrication process.

The multi-scale nature of woven composite materials represents a big challenge in the development of reliable finite element models able to study the different aspects of the material response. At the macroscale level, which is the scale where the whole mechanical part is considered, the fabric is considered as an anisotropic continuous material exhibiting mechanical properties inherited from its meso- and microscale. At the mesoscopic level,

which is the scale of a yarn, the influence of the weave architecture on stress distribution and mechanical properties is considered. Patterns for woven fabrics are defined by the smallest repeating unit cell (RUC), which describes the interlacing of the warp and weft. Fabrics in the dry form are then consolidated with resin via resin transfer molding (RTM) or other manufacturing processes. Among them, the chemical vapor infiltration (CVI) technique has been studied since the 1960s, and has become quite important commercially for high temperature structural applications [2].

Geometric modeling tools combined with finite elements strategies have been developed over the years for the mesoscopic level. A short overview of the most important contributions in the field of thermostructural composites elaborated using the CVI technique, mainly ceramic matrix composites (CMC), is provided herein. TexGen [3] and WiseTex [4] represent the current state-of-the-art in generalized textile modelers. Even though their primary application is in the design and manufacture of fiber-reinforced polymer matrix composites, Nemeth *et* al. compared the two finite element softwares in their capability of modeling various woven architectures of CMC [5]. Tetrahedral meshes were used. Both TexGen and WiseTex were useful for generating solid models of the tow geometry. However, it was concluded that none of the programs at their current state of development was able to provide a complete generalized capability to model a CMC. Moreover, there was a lack of consistency in generating well-conditioned finite element meshes of the tows and matrix since interpenetrations between the meshes were generated. Then, corrective procedures were required. It is important to remark that the main goal of the two softwares is different from both the one of the study carried on in [5] and in the present paper. An interesting method that can be adopted to avoid interpenetration, especially in case of complex preforms, is the Voxel method [6]. The main advantage of this method lies in its simplicity since the meshing can be carried out in few operations whatever is the complexity of the geometry. However, it can provide an extremely rough and mesh-dependent representation of local stress and strain fields, especially at material interfaces, leading to bad predictions of the damage mechanisms.
Another important contribution in the field of the mesoscale modeling of woven CMC was provided by Rao [7]. Rao developed an automated finite element model generator of 2–D textile composites roughly represented, with progressive damage/failure models. It was concluded that continuum damage mechanics can provide a good approximation of the overall response of the material but do not take into account their specificities. In this context, Couégnat *et* al. [8] proposed a multiscale model of the mechanical behaviour of woven ceramic composite materials based on a physical description of the reinforcement geometry of the material and the damage mechanisms. The damage identified experimentally was duplicated in the finite element mesh by creating cracks at the different scales. Couégnat's model represents the most accurate approach currently available in the field of woven ceramic matrix composites. However, an idealized geometry of the textile is adopted at the mesoscale, discretized using rather coarse meshes composed of tetrahedral elements. Moreover, a layer of matrix is introduced between the yarns in contact to simplify the meshing process and avoid interpenetration.
This short overview has pointed out part of the numerical issues commonly encountered using the methodologies proposed in the literature, and the consequent geometry inconsistencies introduced to cope with them. The purpose of this paper is to present a strategy able to avoid some of the aforementioned problems, thus enhancing the current state-of-the-art. In particular, henceforward the attention is restricted to the presentation and validation of the numerical tools developed, and not to the geometrical and mechanical characterization of a real CMC unit cell. Then, a generic two-dimensional RUC of plain weave textile architecture is considered. First, the key points of the strategy are overviewed in section 2, in particular the

steps concerning the geometrical construction of the RUC, and the subsequent generation of the finite element model. Then, the strategy is validated in section 3 considering a generic RUC of a SiC/SiC plain weave textile architecture subjected to uniaxial tension. Finally, the conclusions and the future possible developments will be presented in section 4.

2 Representative unit cell

The present procedure is composed of two main parts. The first part concernes the geometrical modeling of the RUC of a CVI textile structure, and it was developed within the CATIA V5 framework. The second part concerns the finite element modeling and analysis of the RUC, and it was developed within the ABAQUS 6.10 framework. Another possible strategy could be the one of generating both the geometric and the numerical model within the same tool. However, the choice of generating the geometric model using CAD software and the numerical model using finite element software is in the author's idea more appropriate. A summary of the different steps of the procedure is provided below.

2.1 Geometrical model of the RUC.

The first step concerns the geometrical model of the textile reinforcement. Some of the mesoscopic models proposed in the literature have been reviewed in the previous section. A modeling strategy of particular interest is the one proposed by Hivet and Boisse [9]. Hivet and Boisse developed a consistent 3D geometrical model of 2D fabric elementary cells for appropriate finite element simulations of the forming process prior to matrix impregnation. They performed experimental observations using different optical processes to determine real yarn geometry in different cases of yarn structure and weaving. One particularity of this model is that it ensures a realistic contact surface between yarns without interpenetration for all types of weaving. Another particularity of the model is that the section shape varies along the trajectory, so that the influence of contact between yarns on their cross section shape can be taken into account. Moreover, their geometrical model is built using the CAD software CATIA V5. Their geometric model was adopted in the present procedure. Then, the matrix has to be introduced on the fabric. Two hypotheses are formulated. First, it is assumed that the geometry of the reinforcement does not change after the matrix infiltration. Second, the matrix has a constant thickness all over the reinforcement. These assumptions are made to validate the numerical tools, but within CATIA V5 framework is possible to generate any desired geometry for the matrix. Consequently, an entity is created by just adding an extra thickness, equal to the thickness dimension of the layer of matrix, on each yarn. Then, the sheath of matrix is obtained doing a first Boolean operation, i.e. remove operation, between the yarn and the entity generated where the first one is removed from the second one. This procedure is adopted for every yarn in the model. However, this procedure generates interpenetrations between each sheath of matrix and the yarns lying on the perpendicular direction. Then, additional Boolean operations, similar to the previous ones, are necessary between the interfering parts.

2.2 Finite element modeling of the RUC.

In the second step of the procedure the parts generated in CATIA V5 are imported in ABAQUS 6.10 using the '.CatPart' format. This format was preferred to other types of format, i.e. STEP, IGES, because it allows you to store information of the native CAD geometry that are useful for both the assignment of the material properties and the generation of the mesh in

each part of the RUC within the ABAQUS framework. Afterward, the attention is paid to the generation of accurate hexahedral meshes, compatible between the interacting parts of the RUC. Compatibility is extremely important both to avoid interpenetrations and to have more accurate interactions between the different parts of the RUC. The idea is to mesh each part independently because it makes easier the generation of appropriate hexahedral meshes. First, each part is partitioned using planes conceived with the aim of generating subdomains that are easier to mesh using hexahedral regular meshes. The planes of partition used for the sheaths of matrix and the yarns are shown, respectively, in Fig. 1(a) and Fig. 1(b). Then, different meshing techniques of ABAQUS are used on each subdomain. As far as the sheaths of matrix are concerned, both a structured mesh technique and a sweep meshing technique combined with an advancing front algorithm are used [10], see Fig 1. As far as the yarns are concerned, a regular hexahedral mesh is obtained using the sweep meshing technique combined with an advancing front algorithm on each subdomain.

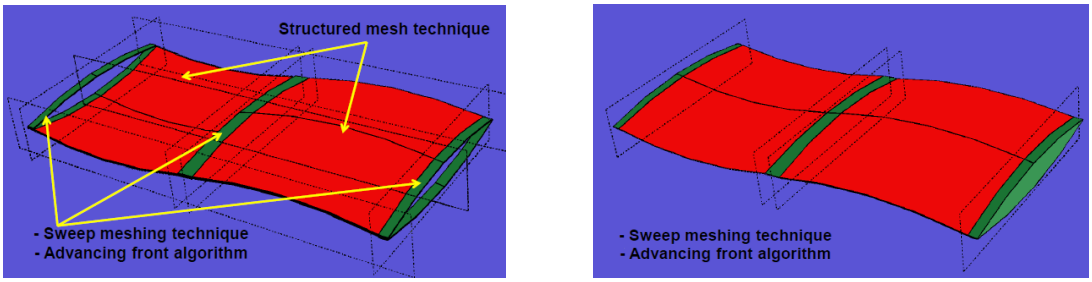

(a) (b)

Figure 1: Partition planes created on the different parts of the RUC for plain textile architecture.

Each mesh is generated in such a way that periodic boundary conditions can be applied using constraint equations. Moreover, all the regions of the RUC in contact have been seeded using the same number of elements and equivalent topology. However, this does not imply that the interacting regions have a compatible mesh. Therefore, a python script [11] was developed to impose compatibility. The idea is the following: a master and a slave surface are defined for each pair of surfaces in contact. Then, each node lying on the slave surface is moved to satisfy compatibility with the closest node on the master surface. This procedure is applied to all the interacting regions in the RUC. Then, the discretized sheaths of matrix are merged to have a better representation of the complete matrix in the RUC. Thus, a single instance is generated for the matrix, see Fig. 2. The yarns are instead kept as independent parts, thus being able to interact with the other parts using, for instance, tie constraints or cohesive laws, i.e. cohesive elements or cohesive surface interactions [10]. A Python script was also developed to impose in-plane periodic boundary conditions on the sides of the RUC. This is done using constraint equations that impose a relative displacement to each pair of nodes sharing the same position on opposite surfaces. For instance, the following constrain equations would be used in case of uniaxial tension in the x-direction, see Fig. 3: $u_1-u_2=\varepsilon_0*L$, $u_3-u_4=0$, where u is the displacement, ε_0 the longitudinal deformation, and L the yarn length.
The mesh quality of the RUC is evaluated using an error estimator output variable based on the strain energy density. It was selected between the set of error indicator output variables provided by ABAQUS Standard for the whole element [10]. These error indicator output variables are computed through the patch recovery technique of Zienkiewicz and Zhu [12]. A finite element model of the RUC of a plain textile architecture obtained using the proposed procedure is shown in Fig. 2.

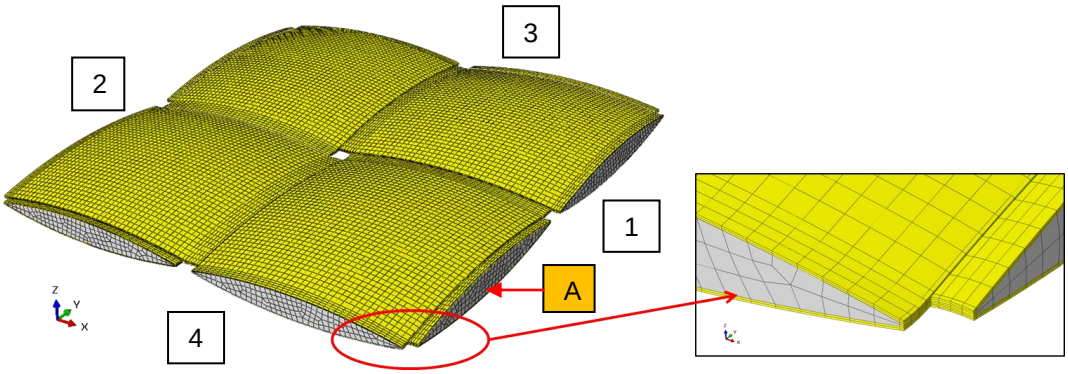

Figure 2: Finite element model of the RUC of a plain textile architecture elaborated using CVI.

2.3 Damage model

A first intra-yarn continuous damage model was introduced on the RUC using a user sub-routine (UMAT) for ABAQUS/Standard [10] to take into account the damage mechanisms commonly encountered in CMCs. A short description of the damage mechanisms and associated model is reported herein. Damage in 2D woven SiC/SiC consists essentially in the formation of transverse cracks in the matrix and associated interface cracking resulting from deviation of the cracks by the tows and the fibers within the tows (also referred to as debonding) [13]. Three main steps can be distinguished during matrix cracking, see Fig. 3. First, cracks initiate at the inter-yarn macropores where stress concentrations exist (strains between 0.025% and 0.12%). Then, cracks form in the transverse yarns and in the interply matrix (strains between 0.12% and 0.2%). Finally, transverse microcracks initiate in the longitudinal tows for strains larger than 0.2%. Ultimate failure is dictated by the fibers.

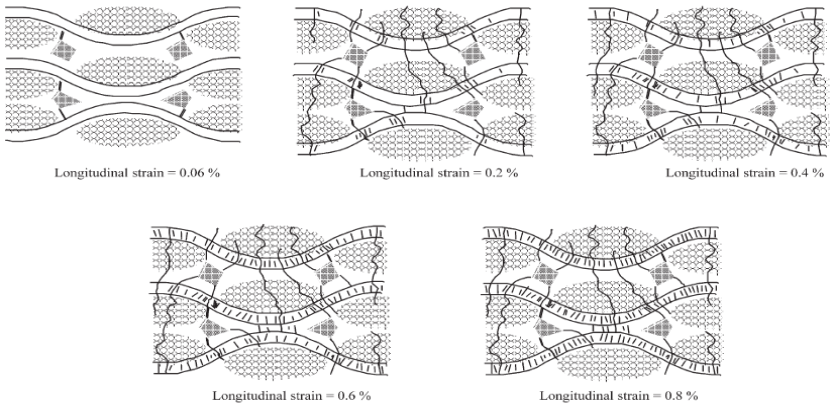

Figure 3: Schematic diagram showing matrix cracking in a 2D SiC/SiC composite during a tensile test [13].

The damage model used in the proposed procedure does not take into account the matrix damage described in the first step. As far as the second step is concerned, cracks in the transverse yarns are taken into account by using a damage model similar to the one proposed at LMT-Cachan for laminated composites [14-15]. Cracks in the longitudinal yarns and associated fiber-matrix debonding are introduced through the use of a model with inelastic deformation, homogenized from the reference fiber scale framework based on shear lag and Weibull theories [16-17]. This homogenization process links the damage variables used on the mesoscale to micromechanical variables such as crack density and crack openings. Fiber breaking is not considered.

3 Numerical results

The proposed procedure was tested considering a generic RUC of a plain weave textile architecture subjected to uniaxial tension in the x-direction, see Fig. 2. The material properties assumed for the yarns and the matrix are based on the study carried on by Lissart and Lamon [18] where they investigated the mechanical properties and statistical parameters of SiC/SiC minicomposites fabricate using CVI. The unit cell edge length is 5.84mm, and the cross section width and maximum thickness are, respectively, 2.68mm and 0.29mm. The thickness of the sheaths of matrix is 20μm. In-plane periodic boundary conditions were assigned on the sides of the RUC (as explained in section 2.2) and tie-constraints were imposed between the interacting parts. Different finite elements of ABAQUS were compared and evaluated in their capability of describing the damage initiation and evolution. The attention was restricted to linear elements since they are, in general, preferred at the quadratic ones when contact interactions are considered [10]. The first mesh was generated using linear hexahedral elements of type C3D8. The mesh quality of the RUC was evaluated using ABAQUS's error estimator output variable based on the strain energy density. A converged solution in the stress-strain curve, leading to reasonable error estimations especially close to the free edges of the RUC, was achieved using a mesh of approximately 90000 elements (≈ 390000 degrees of freedom). It is worth noting that the mesh density assumed here is much finer than the mesh density commonly used in the literature for similar analyses [5]. The stress-strain curve obtained is shown in Fig. 4. This curve was calculated in section A, see Fig. 2, as follows: the stresses are calculated as the ratio between the sum of the nodal longitudinal forces and the cross-sectional area, whereas the deformations as the ratio between (u_1-u_2) and L.

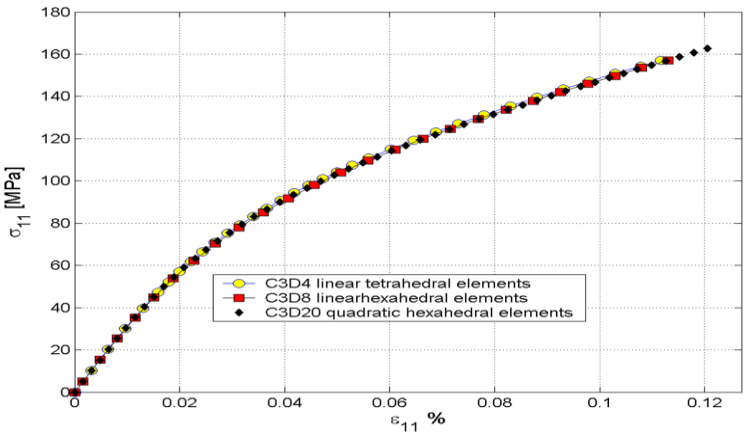

Figure 4: Stress-strain curve obtained using different finite elements.

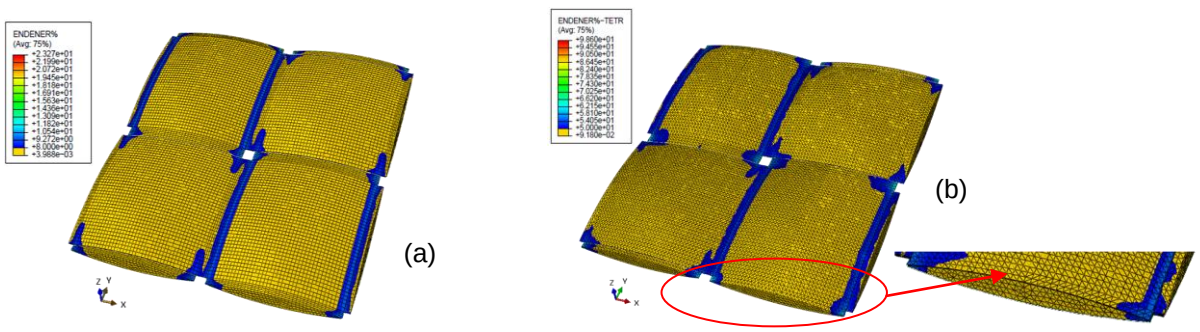

Figure 5: Strain energy density error in the yarns for (a) hexahedral and (b) tetrahedral compatible meshes.

The error estimations obtained in the yarns at the beginning of the non-linear mechanical behavior, i.e. $\sigma_{11} \approx 60$ MPa, for compatible hexahedral meshes are shown in Fig. 5(a). The most important error is encountered close to the macroporosity where it is on average of 20% over a distance of about 5% the in-plane cell dimension. This is due to the singular stress field at the free edges of the macroporosity. On the other regions the error is always less than 8%. Similar results were obtained using linear hexahedral elements of type C3D8I. However, C3D8I elements are preferred to C3D8 elements in presence of complex states of bending [10]. Compatible tetrahedral meshes were also considered. Linear tetrahedral elements of type C3D4 were adopted, and the final mesh had approximately the same number of nodes generated using hexahedral compatible meshes. The stress-strain curve obtained overlaps the one obtained using C3D8 elements, see Fig. 4. However, the estimates of the solution error in the strain energy density are much bigger compared to the ones obtained using C3D8 elements, see Fig. 5b. In most of the regions the error is between 10% and 50%. The error close to the macroporosity is on average of 90% over a distance of about 5% the in-plane cell dimension. Distributions concerning the crack distances in the longitudinal yarns obtained at the end of the analysis using hexahedral and tetrahedral meshes are shown, respectively, in Fig. 6(a) and 6(b). Similar distributions are obtained, even though the error estimations concerning the strain energy density previously shown were quite different. This is because only the local longitudinal stress σ_{11} has an influence on the adopted damage model, and not the complete singular stress field. Even though the sequence of damage mechanisms encountered was similar to the expected one for CMCs, see Fig. 3, the regions of high crack density are not representative of the reality. This is because tie-constrained where used between the parts in contact instead of cohesive interactions. Then, only the macroporosity had an important influence on the damage mechanisms and not, for instance, the interactions between the yarns. It is important to remark that important errors in the strain energy density would have major effects in the prediction of the damage mechanisms in case of cohesive interactions between the parts.

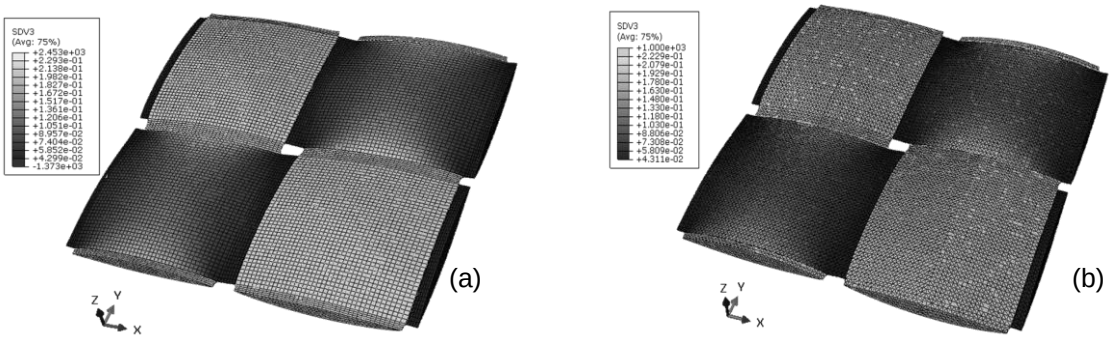

Figure 6: longitudinal crack distances (μm) for, respectively, hexahedral (a) and tetrahedral (b) meshes.

4 Conclusions

The strategy presented in this paper avoids some of the numerical issues and geometry inconsistencies commonly generated using most of the methodologies proposed in the literature regarding the mesoscale modeling of CMCs. For instance, yarn-yarn and yarn-matrix interactions are numerically corrects by imposing mesh compatibility between the interacting parts of the RUC. Moreover, we were able to generate both tetrahedral and hexahedral fine compatible meshes, and using classical error estimators, we found that the former could induce up to 90% error close to stress concentration areas, while with the latter

the error was bounded to 20%. This is of particular interest since most of the meshing strategies proposed in the literature are based on tetrahedrons. In terms of mechanical modeling, the model presented here, though in early stage of development, is already able to reproduce most of the main features of CMCs behavior law. The strategy was illustrated on a generic RUC. Then, certain geometrical assumptions were made to facilitate the presentation of the method and to provide guidelines for further developments. Future research will concern the geometrical and mechanical characterization of more complicate RUCs, e.g. satin and interlock, conceived for thermostructural materials of industrial interest. Great attention will be paid to the development of appropriate cohesive interactions between the parts, and damage models for both the matrix and the yarns.

References

[1] Coupé D. *Woven reinforcements for composites* in "Composite reinforcements for optimum performance", edited by Boisse P., Woodhead Publishing, pp. 89-115 (2011).

[2] Christin F., Design, fabrication, and application of thermostructural composites (TSC) like C/C, C/SiC, and SiC/SiC composites. *Advanced Engineering Materials*, **4**, pp. 895-912 (2002).

[3] Long A.C., Brown L.P. *Modelling the geometry of textile reinforcements for composites: TexGen* in "Composite reinforcements for optimum performance", edited by Boisse P., Woodhead Publishing, pp. 239-264 (2011).

[4] Lomov S.V., *Modelling the geometry of textile reinforcements for composites: WiseTex* in "Composite reinforcements for optimum performance", edited by Boisse P., Woodhead Publishing, pp. 200-238 (2011).

[5] Nemeth N.N., Mital S., Lang J. *Evaluation of Solid Modeling Software for Finite Element Analysis of Woven Ceramic Matrix Composites*, NASA/TM-2010-216250 (2010).

[6] Schneider J., et al. A Meso-FE Voxel Model of an Interlock woven composite in "Proceeding of *International Conference in Composite Materials 17th (ICCM17)*, Edinburgh, Scotland, (2009).

[7] Rao M.P., Pantiuk M., Charalambides P.G. Modeling the Geometry of Satin Weave Fabric Composites. *Journal of composite materials*, **43**, Issue 1, pp. 19-56 (2009).

[8] Couégnat G., Martin E., Lamon J., Carrère N. Multiscale Modeling of the Mechanical Behaviour of Woven Composite Materials in "Proceeding of *International Conference in Composite Materials 17th (ICCM17)*, Edinburgh, Scotland, (2009).

[9] Hivet G., Boisse P. Consistent 3d geometrical model of fabric elementary cell. application to a meshing preprocessor for 3d finite element analysis. *Finite Elements in Analysis and Design*, **42**, pp. 25-49 (2005).

[10] Abaqus Analysis user's manual-abaqus version 6.10.

[11] Abaqus Scripting user's manual-abaqus version 6.10.

[12] Zienkiewicz O.C., Zhu J.Z. A Simple Error Estimator and Adaptive Procedure for Practical Engineering Analysis, *International Journal for Numerical Methods in Engineering*, **24**, pp. 337-357 (1987).

[13] Lamon J. A micromechanics-based approach to the mechanical behavior of brittle-matrix composites, *Composites Science and Technology*, **61**, pp. 2259-2272 (2001).

[14] Cluzel C., Baranger E., Ladevèze P., Mouret A. Mechanical behavior and lifetime modeling of self-healing ceramic-matrix composites subjected to thermomechanical loading in air, *Composites Part A: Applied Science and Manufacuring*, **40**, Issue 8, pp. 976-984 (2009).

[15] Genet M., Marcin L., Baranger E., Cluzel C., Ladevèze P., Mouret A. Computational prediction of the lifetime of self-healing CMC structures, *Composites Part A:Applied Science and Manufacturing*, **43**, Issue 2, pp. 294-303 (2012).

[16] Aveston J., Kelly A. Theory of multiple fracture of fibrous composites, *Journal of Material Science*, **8**, pp. 352-362 (1973).

[17] Curtin W.A. Theory of Mechanical Properties of Ceramic-Matrix Composites, *Journal of the American Ceramic Society*, **74**, Issue 11, pp. 2837-2845 (1991)

[18] Lissart N., Lamon J. Damage and Failure in Ceramic Matrix Minicomposites: Experimental Study and Model, *Acta Materialia*, **45**, Issue 3, pp.1025-1044 (1997).